Journal of Vertebrate Paleontology

ISSN: 0272-4634 (Print) 1937-2809 (Online) Journal homepage: https://www.tandfonline.com/loi/ujvp20

Comparative skull osteology of *Oreomylodon wegneri* (Xenarthra, Mylodontinae): defining the taxonomic status of the Ecuadorian endemic mylodontid

José Luis Román-Carrión & Luciano Brambilla

To cite this article: José Luis Román-Carrión & Luciano Brambilla (2019) Comparative skull osteology of *Oreomylodon wegneri* (Xenarthra, Mylodontinae): defining the taxonomic status of the Ecuadorian endemic mylodontid, Journal of Vertebrate Paleontology, 39:4, e1674860

To link to this article: https://doi.org/10.1080/02724634.2019.1674860

Published online: 13 Dec 2019.

Journal of Vertebrate Paleontology e1674860 (15 pages)

DOI: 10.1080/02724634.2019.1674860

ARTICLE

COMPARATIVE SKULL OSTEOLOGY OF *OREOMYLODON WEGNERI* (XENARTHRA, MYLODONTINAE): DEFINING THE TAXONOMIC STATUS OF THE ECUADORIAN ENDEMIC MYLODONTID

JOSÉ LUIS ROMÁN-CARRIÓN [1,2] and LUCIANO BRAMBILLA *[,3,4,5]
[1]Departamento de Biología, Facultad de Ciencias, Escuela Politécnica Nacional (Quito, Ecuador), Casilla 17-01-2759, Ecuador, joseluis.roman@epn.edu.ec; smilotun@yahoo.com;
[2]Departamento de Paleontología, Facultad de Ciencias Geológicas (UCM) C/ Jose Antonio Novais 2, E-28040, Madrid;
[3]Facultad de Ciencias Bioquímicas y Farmacéuticas, Universidad Nacional de Rosario, Suipacha 531, S2002LRK Rosario, Argentina, lbrambilla@fbioyf.unr.edu.ar;
[4]Consejo de Investigaciones de la Universidad Nacional de Rosario (CIUNR), Rosario, Argentina;
[5]Centro de Estudios Interdisciplinarios de la Universidad Nacional de Rosario (CEI-UNR), Maipú 1065, S2000CGK, Rosario, Argentina

ABSTRACT—The diversity reached by the mylodontids during the Pleistocene has been underestimated in the past. *Oreomylodon wegneri*, the endemic mylodontid of Ecuador, has been considered both a species of *Glossotherium* and a synonym of *Glossotherium robustum*. In this work, we provide a detailed description of abundant *O. wegneri* material and compare it with material of *G. robustum* from Argentina and other mylodontids. The study presented here shows that *O. wegneri* was a mylodontid with a singular cranial morphology, especially in the palate and nasal region and is possibly closer evolutionarily to *Paramylodon harlani* than to the more southern *G. robustum*.

Citation for this article: Román-Carrión, J. L., and L. Brambilla. 2019. Comparative skull osteology of *Oreomylodon wegneri* (Xenarthra, Mylodontinae): defining the taxonomic status of the Ecuadorian endemic mylodontid. Journal of Vertebrate Paleontology. DOI: 10.1080/02724634.2019.1674860.

INTRODUCTION

The Xenarthra are a group of placental mammals of South American origin that presents special evolutionary characteristics (Hoffstetter, 1982; Pascual et al., 1985). The Xenarthra fossil record dates to the Paleocene (Delsuc et al., 2001); however, the actual diversity of fossil taxa is very poorly known for sloths, armadillos, and anteaters.

The Xenarthra-Folivora are grouped in six families: Bradypodidae, Megatheriidae, Megalonychidae, Nothrotheriidae, Mylodontidae, and Orophodontidae (Scillato-Yané, 1977; Gaudin, 2004), but other authors have considered only Megalonychidae, Mylodontidae, Nothrotheriidae, Megatheriidae, and Bradypodidae as valid families (McDonald and De Iuliis, 2008; Slater et al., 2016).

Mylodontidae is the most common and diverse family within the Folivora, with records from late Oligocene to late Pleistocene. Some authors recognize four subfamilies, Mylodontinae, Lestodontinae, Urumacotheriinae, and Scelidotheriinae, whereas others also recognize Nematheriinae and Octomylodontinae (Rinderknecht et al., 2010).

The first remains of Ecuadorian mylodonts were reported by M. Wagner (1860) in the highlands of Sisgun, Chimborazo Province, and were assigned to *Callistrophus priscus* Branco, 1883. Later, Clavery (1925) reported the discovery of a *Mylodon* skeleton in the Cangagua Formation of Cotocollao, north of Quito. Franz Spillmann in 1931 created the species *Mylodon wegneri* and the subspecies *Mylodon robustus punini* based on fossil material collected in 'Quebrada de Chalán' (Fig. 1), next to Riobamba-Chimborazo (Hoffstetter, 1952). Spillmann also reported the presence of many mylodont remains in the eastern valleys of Quito and from the Santa Elena peninsula on the coast (Spillmann, 1931).

In 1952, Hoffstetter transferred *Mylodon wegneri* to *Glossotherium wegneri*, and to the subgenus *Oreomylodon*, which he had established in 1949. Hoffstetter clarified that both Branco's and Claveri's animals belong to *Glossotherium* and that both *Mylodon wegneri* and *Mylodon robustus punini* were poorly described by Spillmann because the first was described from juvenile specimens and the latter from adult material of mylodontids similar to *Glossotherium*. Hoffstetter (1952) noted that all other remains collected by him in the inter-Andean valleys were found only in late Pleistocene strata (Cangagua Formation).

More recently, Dechaseaux (1971) raised Hoffstetter's (1949) subgenus, *Oreomylodon*, to genus status without further justification. The generic status of *Oreomylodon* was followed by Esteban (1996), McDonald (2005), and De Iuliis et al. (2017), but these studies also lack a formal analysis of the genus. Dechaseaux (1971) also recognized that the North American mylodontids should not be included in the genus *Glossotherium*, which was recently supported by McAfee (2009). Ficcarelli et al. (1997, 2003) and Coltorti et al. (1998) assign to the species *G. wegneri* the fossils of mylodontids found in Cangaguas associated with *Haplomastodon waringi* (= *Notimastodon platensis*), *Mazama*, and *Smilodon*.

In 2009, McAfee synonymized *Glossotherium robustum* Owen, 1842, and *G. wegneri* Spillmann, 1931, but recent studies such as Montellano and Román-Carrión (2011) reevaluated the neotype of *O. wegneri* in the paleontology collection of the Colección de Paleontología along with new specimens of *G. wegneri* found in the historic center of Quito and the valley of Chillos (Román-Carrión 2012a, 2012b). The need for an in-depth revision of that synonymy and validation of the genus was recognized.

*Corresponding author.
Both authors contributed equally to this manuscript

Published online 13 Dec 2019

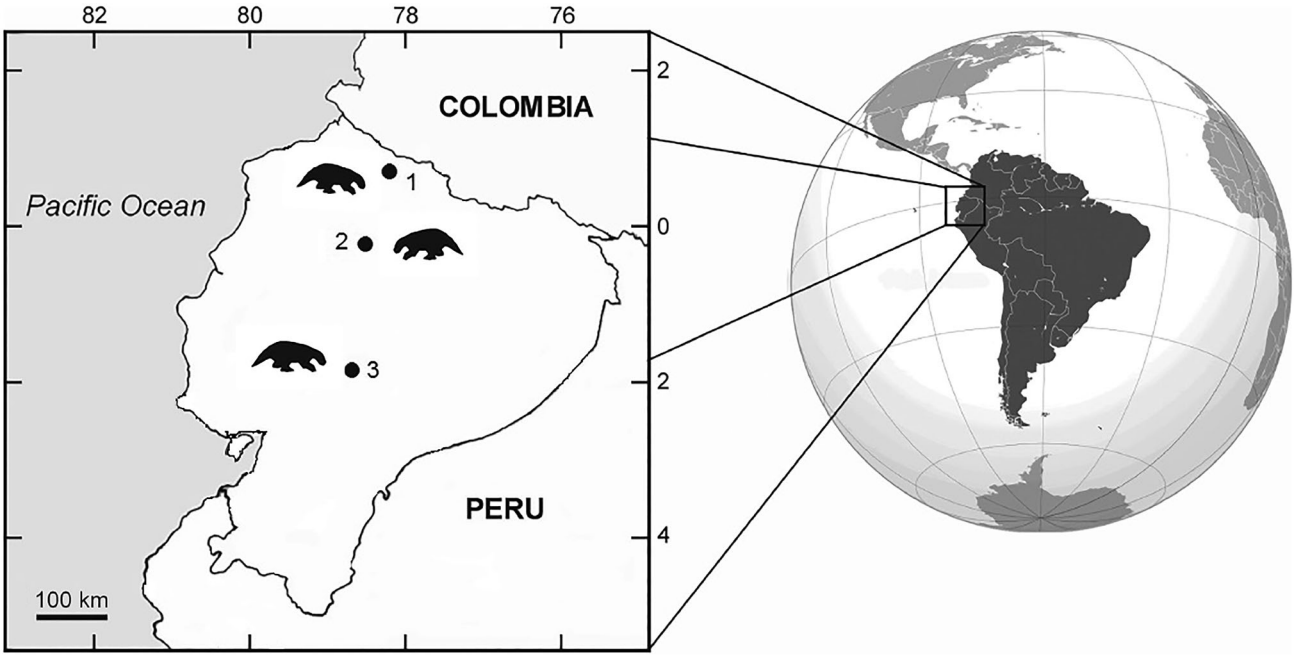

FIGURE 1. Map showing the main fossiliferous localities in Ecuador with remains of *Oreomylodon wegneri*. Modified from De Iuliis et al. (2017). **1**, Quebrada Pistud, Carchi Province; **2**, Quito's valley, Pichincha Province; **3**, Quebrada Chalan, Chimborazo Province.

The taxonomic status and validity of *Oreomylodon wegneri* is relevant in the context of the current knowledge about the Mylodontinae of Ecuador, which also includes *G. tropicorum*, a species that was recently revalidated based on material collected in Corralito (Santa Elena-Ecuador) and in Talara, Perú (De Iuliis et al., 2017).

Oreomylodon wegneri Spillmann, 1931, is frequently found in the north and central parts of the inter-Andean valleys of Ecuador, between 2,450 and 3,100 m above sea level in sediments that have been assigned to the late Pleistocene. New finds of almost complete skeletons in several localities in the Andes (Ficcarelli et al., 1997, 2003; Coltorti et al., 1998; Román-Carrión, 2007, 2012a, 2012b) allow access to previously undescribed material and improve our knowledge of the ontogenetic development and intraspecific variation of the species.

In this work, we compared the skull of *O. wegneri* with skulls of other members of the Mylodontinae. We use the largest number of Mylodontinae specimens studied to date to understand intraspecific variation to better establish the taxonomic position of *O. wegneri*. Our results show that *O. wegneri* is a genus different from the other known mylodontines.

Institutional Abbreviations—AMU-CURS, Colección de Paleontología de Vertebrados de la Alcaldía de Urumaco, Urumaco, Estado Falcón, Venezuela; **EFM**, Herbario-Museo Universidad Central del Ecuador, Quito, Ecuador; **EPNV**, Colección de Paleontología, Escuela Politécnica Nacional, Quito, Ecuador; **FMNH**, Field Museum of Natural History, Chicago, Illinois, U.S.A.; **IMNH**, Idaho Museum of Natural History, Pocatello, Idaho, U.S.A.; **LACM HC**, Los Angeles County Museum of Natural History, Los Angeles, California, U.S.A.; **MACN-Pv**, Sección Paleontología de Vertebrados, Museo Argentino de Ciencias Naturales 'Bernardino Rivadavia,' Ciudad Autónoma de Buenos Aires, Argentina; **MACNC Pv**, Colección Paleontología Vertebrados del Museo de Antropología y Ciencias Naturales de Concordia, Concordia, Corrientes, Argentina; **MARC**, Museo y Archivo Regional de Castelli, Castelli, Buenos Aires, Argentina; **MCA**, Museo Municipal de Ciencias Naturales 'Carlos Ameghino,' Mercedes, Buenos Aires, Argentina; **MCL**, Museu de Ciéncias Naturais da Pontifícia Universidade Católica de Minas Gerais, Belo Horizonte, Brazil; **MD**, Museo Darwin, Punta Alta, Buenos Aires, Argentina; **MECN**, National Institute of Biodiversity, Quito, Ecuador; **MHLC**, Museo Histórico La Campana, Esteban Echeverría, Buenos Aires, Argentina; **MLF**, Museo de Ciencias Naturales 'Florentino Ameghino,' Las Flores, Buenos Aires, Argentina; **MLP**, División Paleontología de Vertebrados, Facultad de Ciencias Naturales y Museo de La Plata, Universidad Nacional de La Plata, La Plata, Buenos Aires, Argentina; **MMCIPAS**, Museo Municipal Centro de Investigaciones Paleontológicas y Arqueológicas de Salto 'José Fernando Bonaparte,' Salto, Argentina; **MMP**, Museo Municipal de Ciencias Naturales de Mar del Plata 'Lorenzo Scaglia,' Mar del Plata, Buenos Aires, Argentina; **MN-V**, Coleção do Museu Nacional do Rio de Janeiro, Brazil; **MNHNM**, Museo Nacional de Historia Natural de Montevideo, Montevideo, Uruguay; **MNHN-BOL**, Museo Nacional de Historia Natural, La Paz, Bolivia; **MNHN SGO**, Museo Nacional de Historia Natural de Chile, Santiago, Chile; **MPAHND**, Museo Particular de Antropología e Historia Natural Los Desmochados, Casilda, Santa Fe, Argentina; **MPRSC**, Museo Paleontológico Real de San Carlos 'Armando Calcaterra,' Colonia, Uruguay; **MPS**, Museo Paleontológico de San Pedro 'Fray Manuel de Torres,' San Pedro, Buenos Aires, Argentina; **MRS**, Museo del Río Salado, Santa Fe, Argentina; **PVL**, Colección de Paleontología de Vertebrados, Instituto Miguel Lillo, Tucumán, Argentina; **ROM**, Royal Ontario Museum, Toronto, Ontario, Canada; **UATF**, Universidad Autónoma Tomás Frías, Potosí, Bolivia; **UCMP**, Museum of Paleontology, University of California, Berkeley, California, U.S.A.; **UF**, Florida State Museum, Florida, U.S.A.; **UNRC-PV**, Universidad Nacional Río Cuarto-Paleontología Vertebrados, Río Cuarto, Córdoba, Argentina; **ZMUC CN**, Zoological Museum, University of Copenhagen, Copenhagen, Denmark.

MATERIALS AND METHODS

Material

Oreomylodon wegneri: EPNV-120 (neotype), EPNV-107 (Paris), EPNV-803, EPNV-5148, EPNV-5202, EPNV-5213,

EPNV-5198, EPNV-4189, MECN S/N, MECN 417, MECN 356, MECN 357, MECN 358, EFM 01; *Archaeomylodon sampedrinensis*: MPS 119; *Bolivartherium codorensis*: AMU-CURS130; *Glossotherium chapadmalense*: MACN-Pv 8675, MMP S-273; *Glossotherium robustum*: MLF 420, MLF 442, MN 3944-V, MACN-Pv 2652, MACN-Pv 11769, MCA 2014, MRS 75, MLP 3-136, MLP 3-137, MLP 3-138, MLP 3-139, MLP 3-140, MLP 3-141, MLP 3-142, MLP 3-144, MLP 3-146, MHLC w/o n, MLP 3-147, MLP 3-178, MLP 3-762, MNHNM 233, MPAHND 9, MARC 15675.a.2/244, MNHN SGO.PV.2; *Glossotherium tropicorum*: ROM 3146; *Glossotherium phoenesis*: MCL 4303/01, MCL 4027; *Lestodon armatus*: MLP 3-3, MLP 3-16, MLP 3-29, MLP 3-30, MACN-Pv 9470, MACN-Pv 10830, MACN-Pv 11687, MPRSC 807; *Lestodon* sp.: MD-98-1; *Mylodon darwinii*: MLF 454, MACNC Pv 2334, FMNH P14288, MLP 36-VIII-12-1, MLP 3-122, MLP 3-762, MLP 3-764, UNRC-PV 002, ZMUC CN 43, MRS 74, MNHN-BOL-V-006470, MMCIPAS B50-2458; *Mylodonopsis ibseni*: MCL 4355; *Paraglossotherium elmollarum*: PVL4326; *Paramylodon garbanii*: UF 10922; *Paramylodon harlani*: LACM HC 692, LACM HC 832, LACM HC 1717-02, LACM HC 1717-04, LACM HC 1717-08, LACM HC 1717-10, LACM HC 1717-22, IMNH 15273, IMNH 23246; *Pleurolestodon acutidens*: MACN-Pv 2953; *Pseudoprepotherium confusum*: UCMP 39957; *Simomylodon uccasamamensis*: MNHN-BOL-V-11731, MNHN-BOL-V-3348, MNHN-BOL-V-3711, MNHN-BOL-V-3726, MNHN-BOL-V-3717, MNHN-BOL-V-3718.

Geometric Morphometric Analysis

The analysis was conducted as in Brambilla and Ibarra (2019). The sample of palates of ground sloths examined was expanded to include *Glossotherium chapadmalense* MMP S-273, *G. robustum* (MNHN SGO.PV.2), *Mylodonopsis ibseni* MCL 4355, *Paramylodon garbanii* UF 10922 (previously considered *Glossotherium chapadmalense* in Robertson, 1976), *Glossotherium tropicorum* ROM 3146, and all the specimens of *O. wegneri* and *Simomylodon uccasamamensis* mentioned in the list of materials. *Lestodon armatus* tend to concentrate the variability of the first component in the diastema between M1 and C1 (Brambilla and Ibarra, 2019) and were not included. The configuration of landmarks was modified by eliminating the landmark on the posterior edge of the palate in order to include those specimens where it is not preserved, such as the holotype of *Mylodonopsis ibseni* and several crania of *O. wegneri*. A new landmark was added on the trailing edge of each M1 to obtain information about the orientation of the major axis of M1, as shown in Figure 8A.

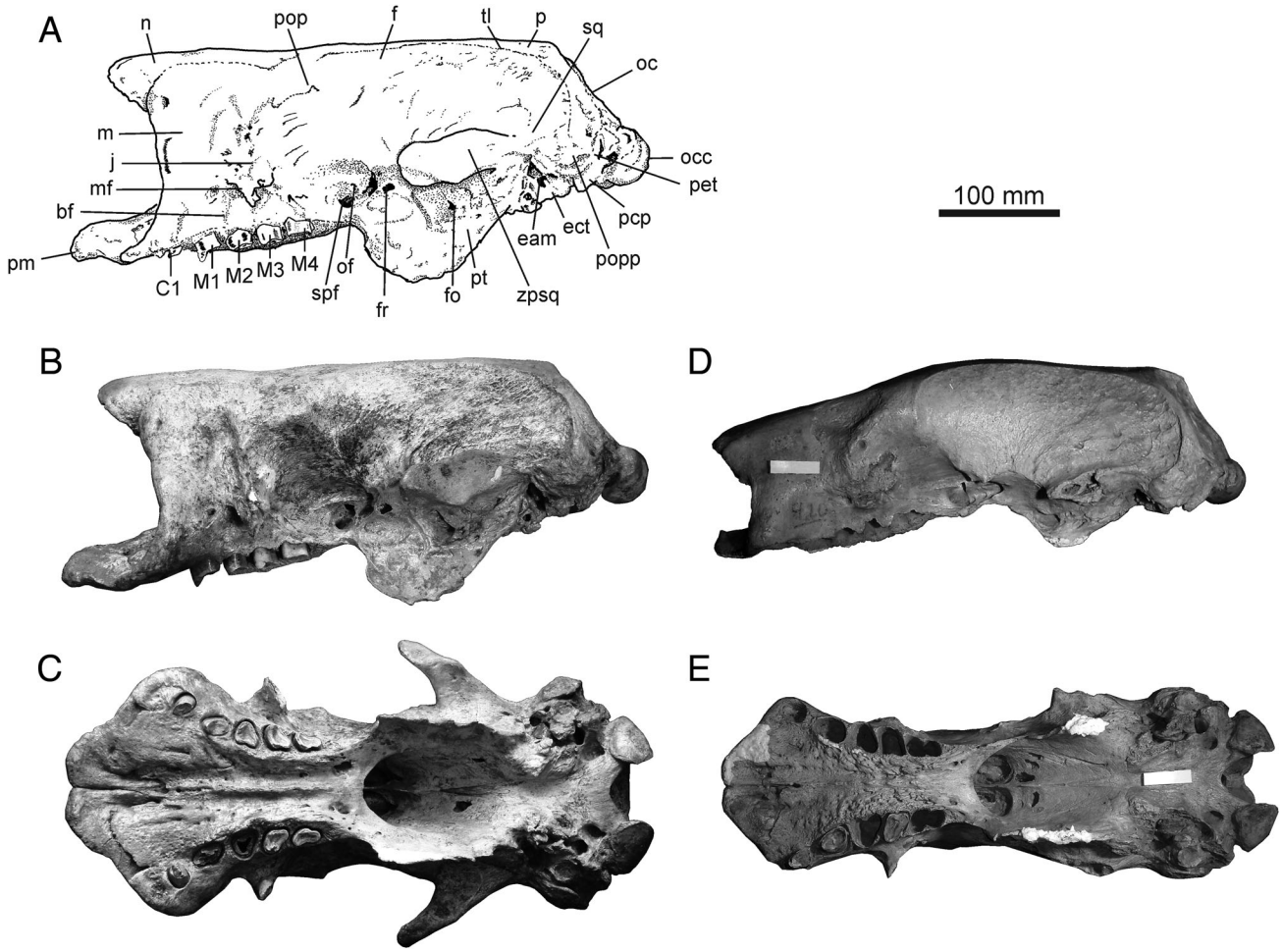

FIGURE 2. Mylodontid crania. **A**–**C**, *Oreomylodon wegneri* EPN V 120: **A**, interpretive drawing; **B**, left lateral view; **C**, ventral view. **D**, **E**, *Glossotherium robustum* MLF 420: **D**, left lateral and **E**, ventral views. **Abbreviations**: **bf**, buccinator fossa; **C1**, upper caniniform; **eam**, external auditory meatus; **ect**, ectotympanic; **f**, frontal; **fo**, foramen ovale; **fr**, foramen rotundum; **j**, jugal; **m**, maxilla; **M1**–**4**, first to fourth upper molariforms; **mf**, maxillary foramen; **n**, nasal; **oc**, occipital; **occ**, occipital condyle; **of**, optic foramen; **p**, parietal; **pcp**, paracondylar process of the exoccipital; **pet**, petrosal; **pm**, premaxilla; **pop**, postorbital process; **popp**, paroccipital process of the petrosal; **pt**, pterygoid; **spf**, sphenopalatine foramen; **sq**, squamosal; **tl**, temporal line; **zpsq**, zygomatic process of squamosal.

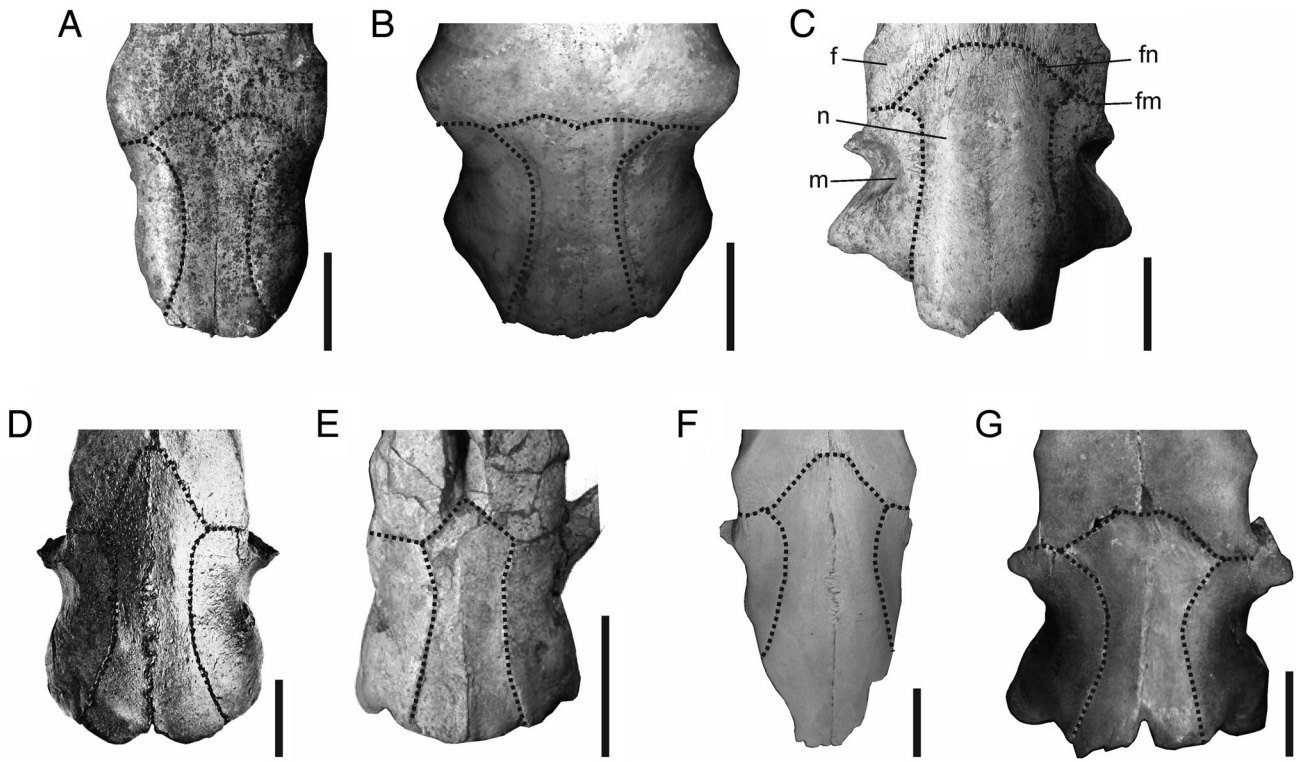

FIGURE 3. Mylodontid frontonasal and frontomaxillary sutures. **A**, *Glossotherium chapadmalense* MMP S-273; **B**, *Glossotherium robustum* MLF 442; **C**, *Oreomylodon wegneri* EPNV-120; **D**, *Paramylodon harlani* LACM HC 642 (modified from Stock, 1907); **E**, *Simomylodon uccasamamensis* MNHN-BOL-V-3726 (modified from Boscaini et al., 2018a); **F**, *Mylodon darwinii* MLF 454; **G**, *Lestodon armatus* MACN-Pv 11687 (modified from Czerwonogora and Fariña, 2012). **Abbreviations**: **f**, frontal; **fm**, frontomaxillary suture; **fn**, frontonasal suture; **m**, maxilla; **n**, nasal. Scale bars equal 50 mm.

Phylogenetic Analysis

A phylogenetic analysis was carried out in TNT (Goloboff et al., 2008), using a data matrix modified from that of Gaudin (2004) and similar to those of Boscaini et al. (2018a) and Brambilla and Ibarra (2019); see Appendix 1. The mylodontids of the Miocene–Pleistocene and the non-mylodontids *Hapalops* and *Bradypus*, along with the armadillo *Euphactus* and the anteaters *Cyclopes*, *Tamandua*, and *Myrmecophaga*, were used from the original matrix of Gaudin (2004). We also included *Simomylodon uccasamemensis*, *Baraguatherium takumara*, *Archaeomylodon sampedrinensis*, and *Oreomylodon wegneri*.

The data were analyzed through a traditional search with 10,000 replications, using tree bisection reconnection algorithm and collapsing the trees after search. Bremer and bootstrap support values were calculated using TNT.

Basicranium

The anatomy of the basicranium of *O. wegneri* was compared with that of *Glossotherium robustum* following the previous works of Patterson et al. (1992), Gaudin, (1995, 2004), De Iuliis et al. (2011), Boscaini et al. (2018b), and Brambilla and Ibarra (2019).

SYSTEMATIC PALEONTOLOGY

XENARTHRA Cope, 1889
PILOSA Flower, 1883
FOLIVORA Delsuc et al., 2001
MYLODONTIDAE Gill, 1872
MYLODONTINAE Gill, 1872
OREOMYLODON Hoffstetter, 1949

OREOMYLODON WEGNERI (Spillmann, 1931)
(Figs. 2A–C, 5A, 6, 7A–G, 8A, 9A–D, 12)

Extended Diagnosis—Upper tooth rows more divergent toward the anterior region than in *Glossotherium robustum*. Separation of the tooth rows at the level of M4 greater than 3 times the length of M1. Nasals higher than the frontal as in *Mylodon darwinii*. Diastema between M1 and C1 as in *G. robustum*. Basicranium anteroposteriorly short as in *Paramylodon harlani* and *G. robustum* distinguishes it from the more elongated basicranium of *M. darwinii* and *Archaeomylodon sampedrinensis*. Paroccipital process of petrosal and occipital condyles are prominent. Frontonasal suture at level of postorbital processes. Blunt posterior margins of nasals. Parallel dorsal and ventral edges of horizontal mandibular ramus.

DESCRIPTION

Cranium

The cranium is robust as in *Lestodon armatus* and *Glossotherium robustum* (Fig. 2). In dorsal view, the sagittal crest of *Oreomylodon wegneri* is wide. The temporal lines are strongly separated toward the anterior region of the frontal to contact the postorbital processes as in *L. armatus*. The postorbital processes are developed as in *L. armatus*. The anterior edge of the nasals is a 'V' shape as in *Paramylodon harlani*, unlike the blunt nasal of *G. robustum* and *G. chapadmalense* Kraglievich, 1925 (Fig. 3). The posterior edges of the nasals have a blunt tip shape as in *L. armatus*, *Mylodon darwinii*, and *P. harlani*, whereas in *G. robustum* and *G. chapadmalense* the posterior edge of nasals have a fishtail shape (Fig. 3).

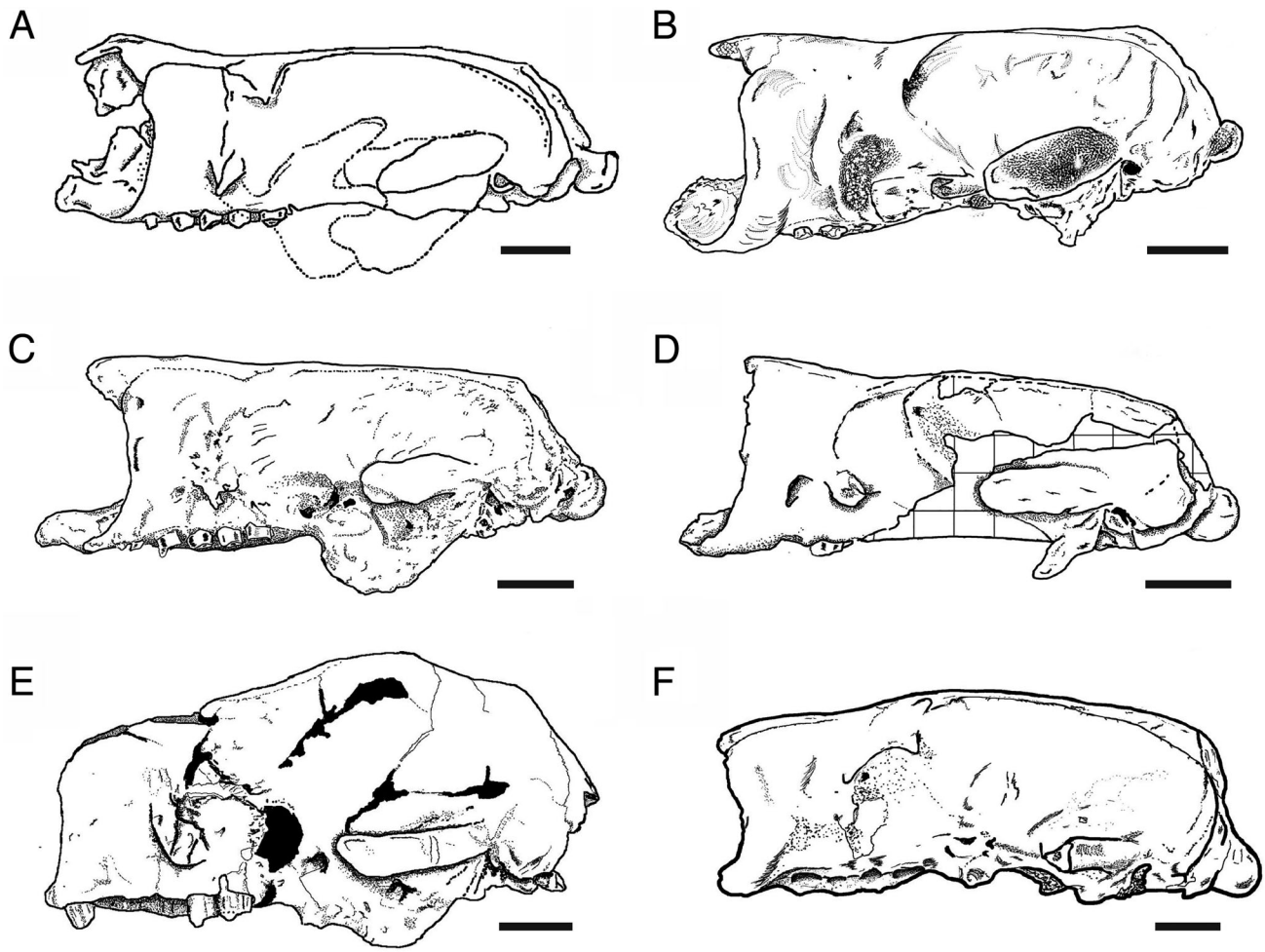

FIGURE 4. Mylodontid crania in lateral view. **A**–**D**, *Oreomylodon wegneri*: **A**, EPNV-107; **B**, EPNV-5213; **C**, EPNV-120; **D**, EPNV-5202; **E**, *Glossotherium tropicorum* ROM 3146 (modified from De Iuliis et al., 2017); **F**, *Glossotherium robustum* MARC 15675.a.2/244. Scale bars equal 50 mm.

In dorsal view, the maxilla expands abruptly in front of the preorbital constriction until reaching a greater width than at the postorbital processes, in contrast to the mediolaterally less wide maxilla of *P. harlani* and *G. robustum*. The widening of the maxilla occurs to a greater extent at its base, and this produces a triangular nasal opening in the anterior view.

In lateral view, the roof of the cranium formed by the parietal and frontal is flattened, in contrast to the more rounded shape in *G. tropicorum* (Fig. 4). A slight prefrontal depression is observed, like in other mylodontins, and toward the anterior region the nasals have an elevation in their extension above the maxilla, as in *M. darwinii* and *Pleurolestodon acutidens*, in contrast to *G. robustum* and *L. armatus* in which the lowest position of the rostrum is with respect to the frontal bone (Figs. 2, 4). The surface of the nasals is markedly convex transversely but slightly convex longitudinally, so it does not form a well-defined dome as in *M. darwinii*.

The nasal bones project anteriorly to the anterior border of the maxilla as in *M. darwinii*, whereas in *G. robustum* the nasal bones extend nearly to the same level of the anterior border of the maxilla (Figs. 2D, 4).

The anterior view of *O. wegneri* shows a widening of the rostrum at the base of the maxilla and lateral walls, and the bulging of the nasals over the maxilla becomes more visible (Fig. 5). The dorsal meatus of *O. wegneri* is huge compared with the same structure in *G. robustum*. This is almost separated from the middle meatus due to the development of the dorsal nasal turbinal; it is cylindrical with a conical opening. The dorsal lamina of the ventral turbinal is smaller than in *G. robustum*, although the ventral turbinal and the ventral meatus are similar in size. In the upper part of the vestibule in the nasal cavity, two vestibular plates are present. The nasal septum divides the cavity and in some individuals it has a pronounced deviation forming a 'S' shape, whereas it is straight in *G. robustum*. The nasal septum of *O. wegneri* is articulated directly with the maxilla, forming the base of the nasal fossa, which is also very broad. A prenasal bone is articulated with the nasals (Hoffstetter, 1949). Figure 5 shows a rounded articular surface for the prenasal bone in *O. wegneri*, which is absent in *G. robustum*, *P. harlani*, *L. armatus*, and *P. acutidens*. The prenasal bone is also present in *M. darwinii*, although in *O. wegneri* it is described as a small rhomboid element by Hoffstetter (1949) and in *M. darwinii* it forms an arch that contacts the nasals and the premaxilla (Kraglievich, 1934).

In posterior view, the occipital region is elliptical, and dorsoventrally depressed (Fig. 6) as in *G. robustum*, unlike the more circular occipital of *P. harlani*, *L. armatus*, and *M. darwinii* (Brambilla and Ibarra, 2018). The size of the foramen magnum is variable, as is also observed in *G. robustum*, *L. armatus*, and *M. darwinii* (Brambilla and Ibarra, 2018). In lateral view, the occiput of *O. wegneri* is significantly more inclined than in *G. robustum* (Figs. 2, 4)

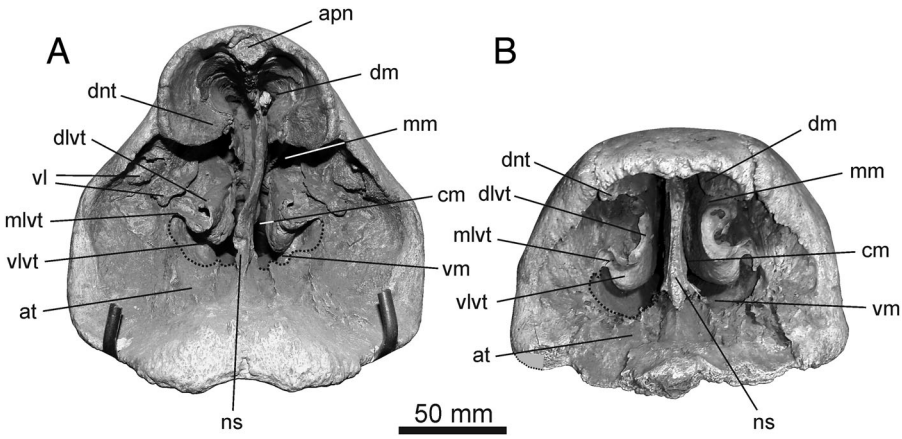

FIGURE 5. Mylodontid nasal regions. **A**, *Oreomylodon wegneri* EFM 01; **B**, *Glossotherium robustum* MLF 442. **Abbreviations**: **apn**, articular surface for prenasal bone; **at**, atrium; **cm**, common meatus; **dlvt**, dorsal lamina of the ventral turbinal; **dm**, dorsal meatus; **dnt**, dorsal nasal turbinal; **mlvt**, main lamina of the ventral turbinal; **mm**, middle meatus; **ns**, nasal septum; **vl**, vestibular lamina; **vlvt**, ventral lamina of the ventral turbinal; **vm**, ventral meatus.

In a lateral view, the palate is straight or almost straight between the molariforms as in *Archaeomylodon sampedrinensis*, whereas in *G. robustum*, *P. harlani*, and *L. armatus* the palate is more convex. The zygomatic process of the squamosal becomes wider forward and leans toward the ventral region. The lacrimal anteriorly is one-third the size of the lacrimal foramen of *G. robustum*. The sphenopalatine, the ovale, and the rotundum foramina are located behind the M4, approximately at the maxillary foramen level. The relative position between these foramina and their size are similar to those of *G. robustum*.

In ventral view, the ventral edge of the maxillary foramen is reduced to a small bony bridge, as noted by Hoffstetter (1949). In contrast, the maxillary foramen is well defined ventrally in *G. robustum*, and in *M. darwinii* the foramen is deeply inserted in the maxilla.

The anterior divergence of the tooth rows stands out, and the maximum width of the maxilla occurs at the level of the caniniform (C1). The dentition composition is the typical 5/4 formula in Mylodontinae. The caniniforms have an elliptical cross-section, generally displaced labially; the major axis of C1 adopts diverse angles that vary from a perpendicular position to the tooth row to a divergent orientation, with the anterior edge labially oriented (Fig. 7). In some specimens, the C1 is reduced, as was noted by Hoffstetter (1949).

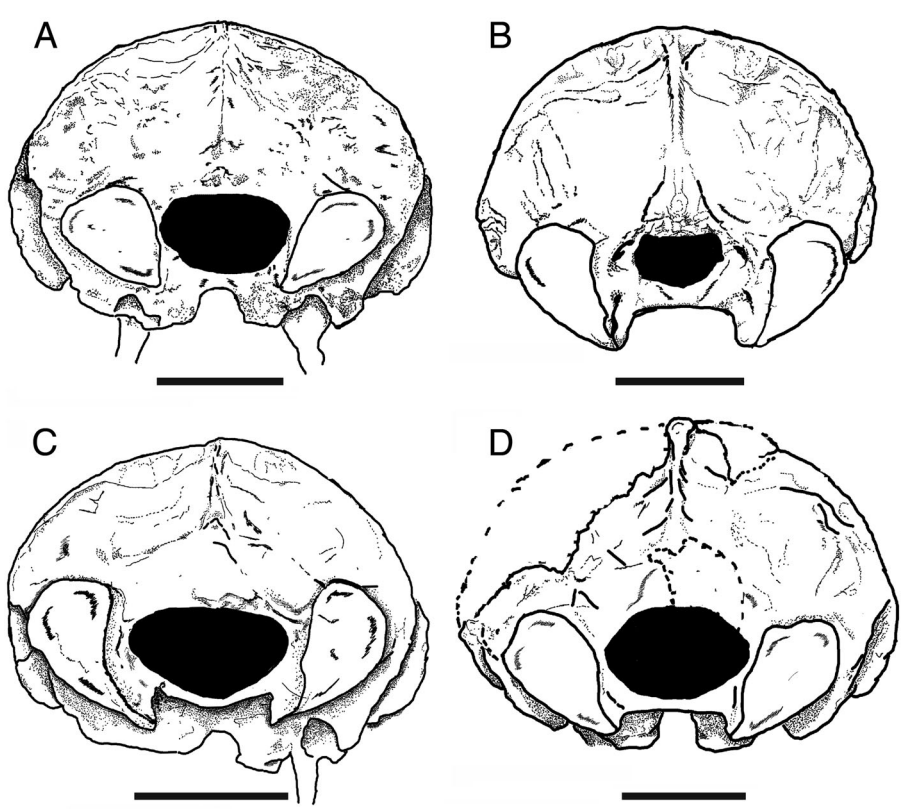

FIGURE 6. Occipital region of *Oreomylodon wegneri*. **A**, EPNV-5213; **B**, EFM 01; **C**, EPNV-5202; **D**, EPNV-5148. Scale bars equal 50 mm.

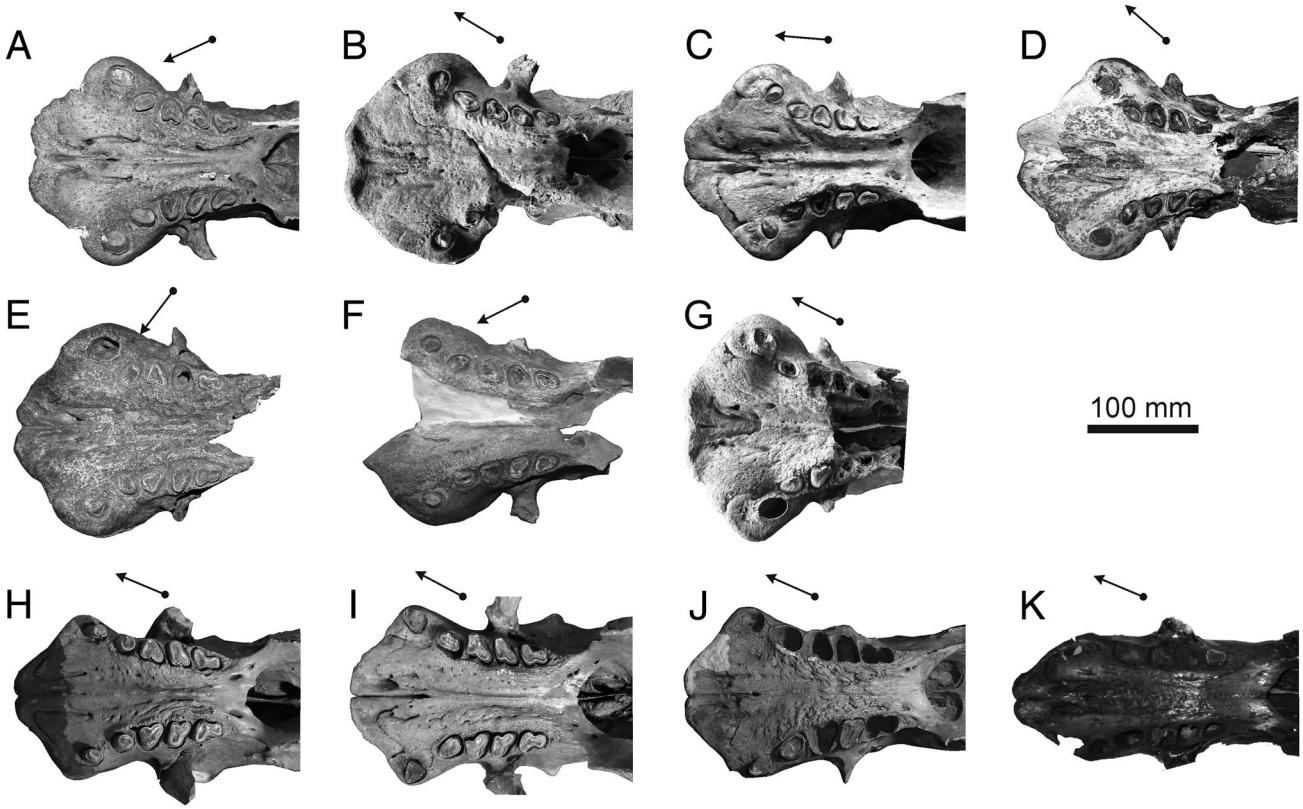

FIGURE 7. Palates of the late Pleistocene mylodontids. **A**–**G**, *Oreomylodon wegneri*; **H**–**J**, *Glossotherium robustum*; **K**, *Paramylodon harlani*. The arrows show the orientation of the major axis of the molariform M1.

The first molariform (M1) is elongated, and its orientation is also variable among the specimens, as is the case with C1, with the anterior edge oriented from lingual to labial. There is no correlation between the degree of rotation of C1 and M1 and the variation in the orientation of the major axis of M1. This molariform in specimen MECN 356 is displaced lingually with respect to the orientation of the tooth row. The M1 is similar in size to M2, but smaller in some specimens. The M2 and M3 are subtriangular in shape as in *P. harlani*, *G. robustum*, and *M. darwinii*, whereas M4 is bilobed, with the anterior lobe larger than the posterior lobe. Although the M3 is subtriangular, the anterior lobe is poorly defined in most specimens and the lingual side is shorter than that of the M2; M3 has smaller area than M2 (Fig. 7).

The palate is concave transversely, and the concavity extends between M1 and M4, interrupted by the elevation of the central suture of the maxilla between M1 and M4.

The premaxilla extends across almost the entire anterior region of the maxilla and extends posteriorly in the palate to the level of the anterior border of C1.

The basicranium of *O. wegneri* is short anteroposteriorly as in *L. armatus*, *G. robustum P. harlani*, and *S. uccasamamensis*, and unlike the elongated basicranium observed in *M. darwinii* and *A. sampedrinensis*. The occipital condyles of *O. wegneri* are strikingly projected and noticeably far from the basicranium in comparison with the condition in *G. robustum* (Fig. 8).

The paroccipital process of the petrosal (= mastoid process of squamosal of Patterson et al., 1992) is more developed, prominent, and laterally expanded toward the posterior region in *O. wegneri* than in the rest of the Mylodontinae. This process produces the remarkable widening of the basicranium noted by Hoffstetter (1949). The stylohyal fossa is rough, broad anteriorly, narrower at its posterior edge, and more rounded in *G. robustum* (Boscaini et al., 2018b). The anterior edge of the jugular foramen is located at the level of the posterior border of the stylohyal fossa.

The entotympanic is massive and broader posteriorly and narrower in the anterior region, as in *G. robustum*. This is perhaps a product of the greater development in that portion of the basicranium that is reflected in the size of the paroccipital process of the petrosal, the anterior region of the stylohyal fossa, and posterior region of the entotympanic. The zygomatic process of the squamosal moves notably away from the cranium in comparison with that in *G. robustum*. The ectotympanic of *O. wegneri* is similar to that of *G. robustum*, but smaller in EFM 01 (Fig. 8).

Mandible

In dorsal view, the spout is well marked, and a concave edge separates it from the tooth rows. The edge on the spout at the mandibular symphysis is concave (Fig. 9). The outer edge of the symphysis forms a small keel in some specimens. The c1 is displaced laterally, and a small diastema exists between c1 and m1. The shape of the teeth does not differ significantly from those of *P. harlani*, *G. robustum*, and *S. uccasamamensis*. The m3 has an anterior lobe and a bridge of similar thickness to that of the anterior lobe and connects a small posterior lobe that is hardly differentiated in some specimens (Fig. 9). This differs from the marked posterior lobe of *P. harlani*, *G. robustum*, and *S. uccasamamensis*.

In lateral view, the lower edge of the mandible is slightly concave. The height of the horizontal mandibular ramus is constant at the level of the tooth row and becomes thinner toward the anterior region, between c1 and the mandibular symphysis. In *G. robustum*, the horizontal mandibular ramus shows a height loss toward the anterior region between m3 and m1 (Fig. 9E, F). The coronoid process has a height similar to the height of the horizontal mandibular ramus at the level of m3.

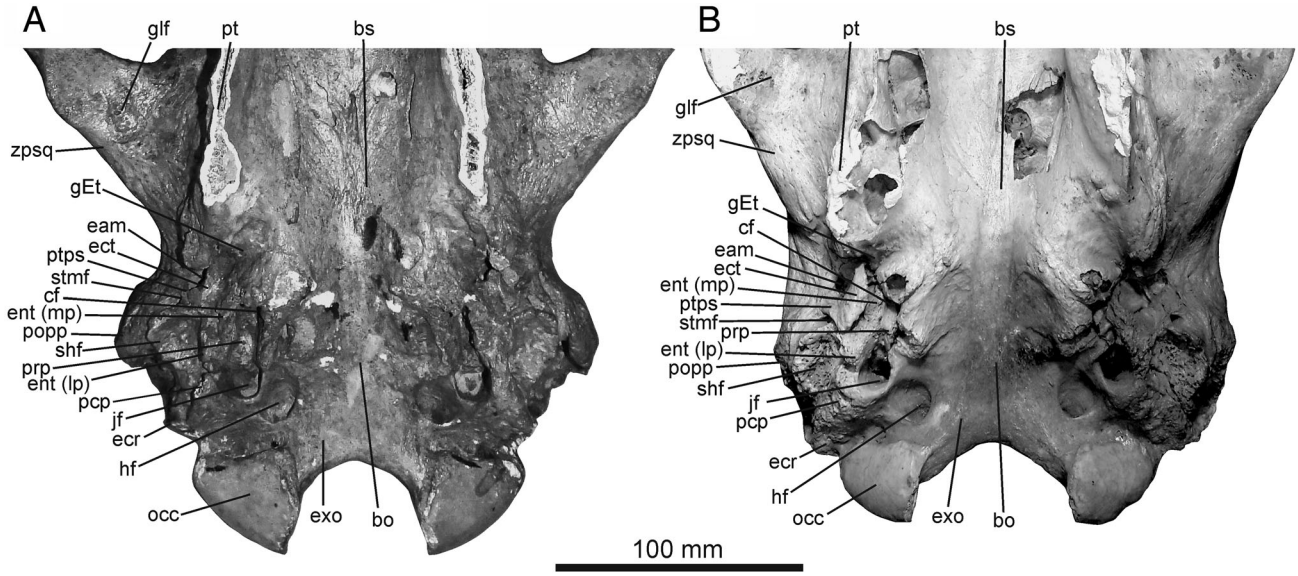

FIGURE 8. Mylodontid basicrania. **A**, *Oreomylodon wegnerai* EFM 01; **B**, *Glossotherium robustum* MLF 420. **Abbreviations**: **bo**, basioccipital; **bs**, basisphenoid; **cf**, carotid foramen; **eam**, external auditory meatus; **ecr**, exoccipital crest; **ect**, ectotympanic; **en (lp)**, entotympanic (lateral plate); **ent (mp)**, entotympanic (medial plate); **exo**, exoccipital; **gEt**, groove for the Eustachian tube; **glf**, glenoid fossa; **hf**, hypoglossal foramen; **jf**, jugular foramen; **occ**, occipital condyle; **pcp**, paracondylar process of the exoccipital; **popp**, paroccipital process of petrosal; **prp**, promontorium of petrosal; **pt**, pterygoid; **ptps**, posttympanic process of squamosal; **shf**, stylohyal fossa; **stmf**, stylomastoid foramen; **zpsq**, zygomatic process of squamosal.

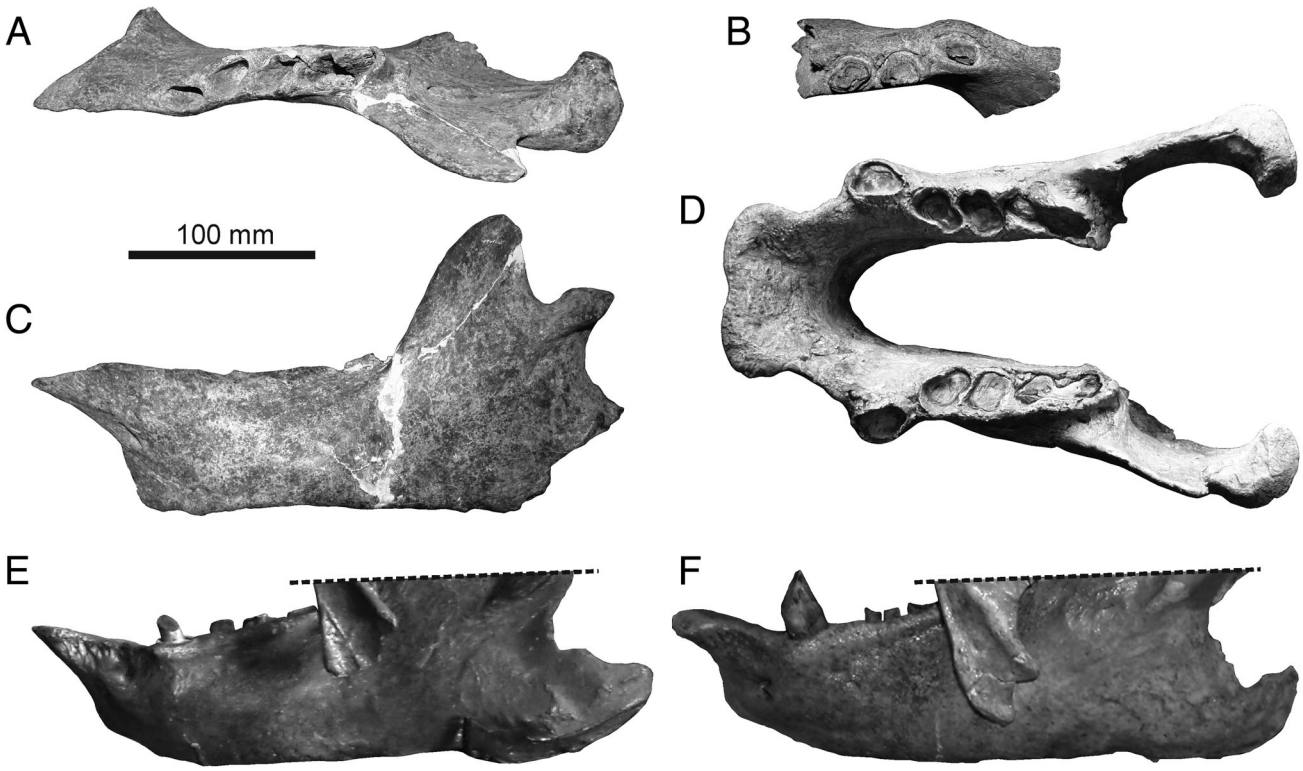

FIGURE 9. Mylodontid mandibles. **A**–**D**, *Oreomylodon wegneri*: **A**, MECN 357, left hemimandible in lateral view; **B**, MECN 358, fragment of left hemimandible; **C**, MECN 357, mandible in occlusal view; **D**, EPNV-5260, complete mandible in occlusal view. **E**, **F**, lateral views of *Glossotherium robustum* mandibles: **E**, MHLC w/o n; **F**, MCA 2014 (modified from Arzani et al., 2014).

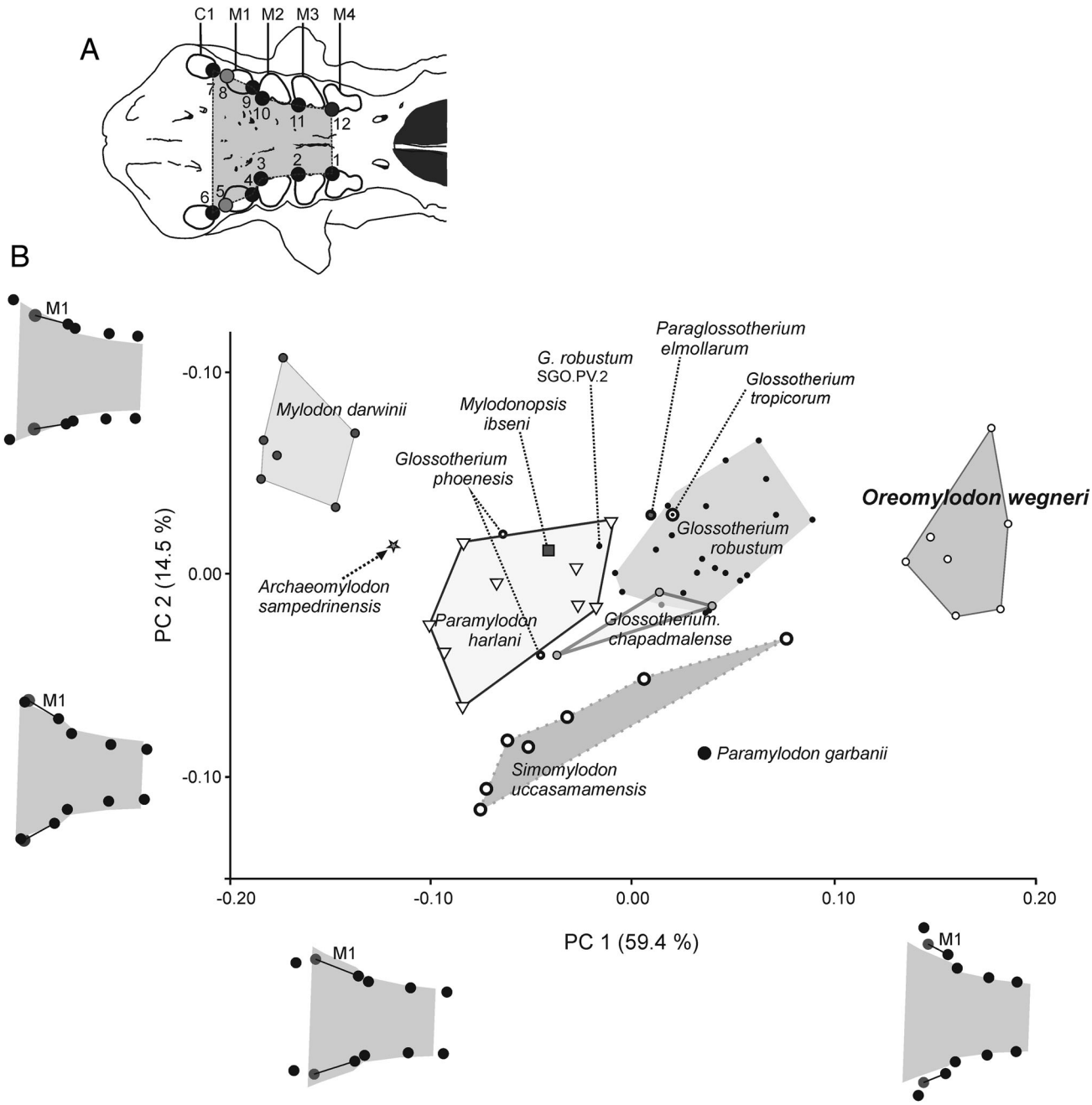

FIGURE 10. Morphogeometric analysis of the palate of Pliocene–Pleistocene mylodontids. **A**, landmark configuration. **B**, PCA from the landmark coordinates.

RESULTS

Geometric Morphometric Analysis

The first principal component (PC1) summarizes 59.4% of the variation and PC2 14.5% (Fig. 10). Both principal components allow for clear differentiation of *Oreomylodon wegneri* from the other mylodontines analyzed. The configuration of the palate of *O. wegneri* differs from that of *Mylodon darwinii* mainly due to the degree of divergence of the tooth rows. The palate of *O. wegneri* is more similar in shape to that of *Glossotherium robustum*, although it can be differentiated clearly by the degree of divergence between C1 and M1, the length of M1 (more reduced in *O. wegneri*), and the greater distance between the tooth rows in *O. wegneri*.

The *O. wegneri* specimens produce both positive and negative values of PC2, mainly due to the variability in the size of the diastema between C1 and M1 as well as to the separation of the tooth rows at the level of M3–M4. The Miocene and Pliocene mylodontids are located at lower values of PC2, characterized by divergent tooth rows in the anterior region of the palate, narrow space between them at the level of M3–M4, and a diastema between C1 and M1 that varies between moderate and nonexistent.

Phylogenetic Analysis

A single tree was obtained in the phylogenetic analysis that included Miocene–Pleistocene mylodontids and other xenarthra as outgroups (tree length = 764, consistency index = 0.652,

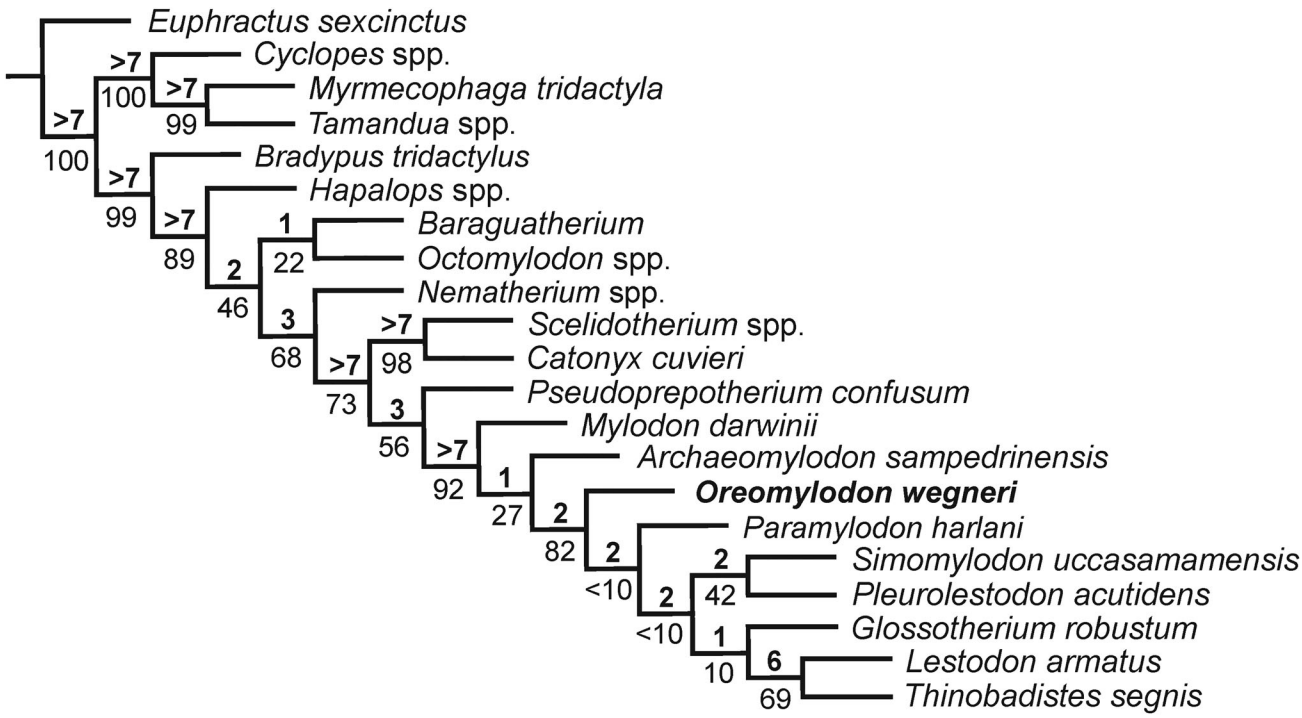

FIGURE 11. Phylogenetic tree obtained from Gaudin (2004) cranial data matrix including *Oreomylodon wegneri*.

retention index = 0.928) (Fig. 11). The tree was similar to that obtained by Brambilla and Ibarra (2019). Although *O. wegneri* was in an intermediate position between *M. darwinii*, *Archaeomylodon sampredrinensis*, and *Paramylodon harlani*, the Bremer and bootstrap support values indicate that it is phylogenetically closer to *P. harlani* than to the more basal mylodontids. It is also noted that it was not recovered in the phylogenetic tree as a sister group of *G. robustum*.

Ontogenetic Comments

The specimen EPNV-5298 (Fig. 12) is a juvenile of *O. wegneri* judging by the presence of conical teeth, open cranial sutures, and small size. It was found in the historic center of the city of Quito among the remains of other adult specimens (Román-Carrión, 2012a). The most relevant characteristics of the species, such as nasals higher than the frontal, nasals longer than the maxilla, divergent and widely separated tooth rows, and constant height of the horizontal mandibular ramus, are already present. The preorbital region is comparatively shorter than in adult specimens. In anterior view, the nasal region is triangular and the dorsal meatus is also very developed as in adults. In the maxilla, C1, M1, and M2 are preserved, and like the teeth of the mandible they exhibit little wear, to a lesser extent in C1/c1 and M1/m1. The occipital region shows clear signs associated with the juvenile stage, such as the weak insertion marks of the muscles and occipital condyles in development, which is evident from the rough surface denoting the presence of cartilage over it, as is common in other juvenile mylodontids (Brambilla and Ibarra, 2018).

Intraspecific Variation

The torsion of C1 and the torsion and alignment of M1 with the rest of the tooth row are undoubtedly points of greater intraspecific variability in *O. wegneri*. Also, in the maxilla, some specimens (EPNV-5202 and EPNV-5213) in ventral view show a depression in the diastema between C1 and M1 (Fig. 5B, G). At the same time, in lateral view, a fold of the maxilla surrounds the root of C1 and the anterior region of the buccinator fossa is below the fold of C1. This could be a product of heterochronous development of the maxilla that is not observed in any other mylodontids.

The sagittal crest shows variable width, although it is generally wide, whereas in *G. robustum* the variation in the width of the sagittal crest is more evident (Fig. 13). The occipital region is dorsoventrally compressed (Fig. 6) as in *G. robustum* (Brambilla and Ibarra, 2018) and slightly higher in EFM 01, contrary to the more rounded occipitals of *M. darwinii*, *P. harlani*, *G. phoenesis*, and *G. tropicorum*. The size of the foramen magnum is variable, as previously observed in other Quaternary mylodontids (Brambilla and Ibarra, 2018).

DISCUSSION

The plesiomorphic condition at the frontonasal suture in mylodontids is the 'U' or 'V' shape (posterior edge of nasals in a blunt tip shape) condition as observed in *Oreomylodon wegneri* or *Mylodon darwinii*. However, an evolutionary novelty in the posterior shape of the nasals is the 'fish tail' that is only present in the lineage of *Glossotherium* from the southern region of South America at least from the Pliocene, as seen in *Glossotherium chapadmalense* and continued in *Glossotherium robustum* until the late Pleistocene. The presence of this character only in the southern *Glossotherium* allows us to speculate that *G. chapadmalense* is not the common ancestor of the North American genus *Paramylodon*, which retains the typical shape of the posterior edge of the nasals. For this reason, there could be other lineages present outside the southern region of South America that may have migrated into North America. Following this reasoning, *G. chapadmalense* would not be the ancestor of

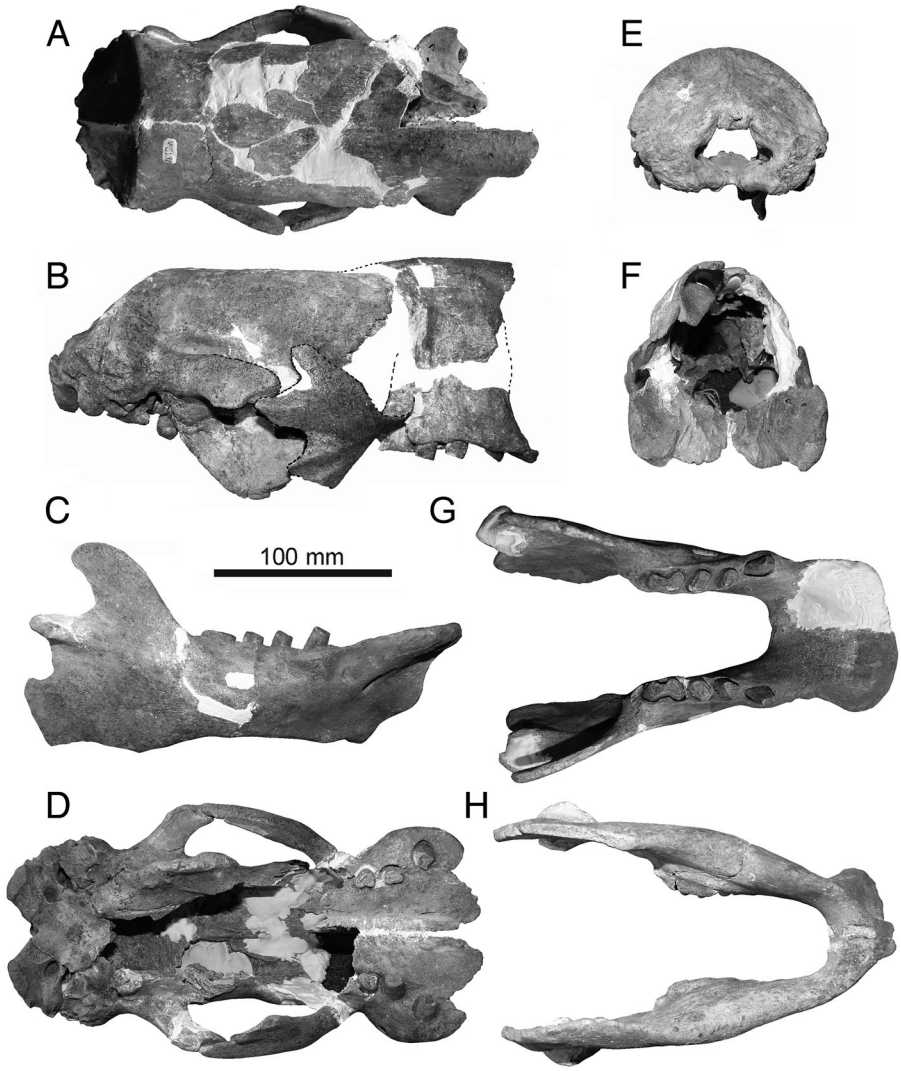

FIGURE 12. Juvenile skull of *Oreomylodon wegneri* EPNV-5298. **A**, dorsal view of the cranium; **B**, lateral view of the cranium; **C**, right lateral view of the mandible; **D**, ventral view of the cranium; **E**, occipital view of the cranium; **F**, anterior view of the cranium; **G**, dorsal view of the mandible; **H**, ventral view of the mandible.

other mylodontines such as *O. wegneri*, *G. phoenesis* (Cartelle et al., 2019), or *G. tropicorum* Hoffstetter, 1952, that also exhibit the plesiomorphic condition of the posterior nasal region.

Regarding the dentition, *O. wegneri* possesses the five teeth in the maxilla as is typical of other ground sloths such as *G. robustum* or *Paramylodon harlani* and Miocene–Pliocene genera such as *Pleurolestodon* and *Simomylodon*. In these taxa, the first tooth is modified into a caniniform and the subsequent teeth are molariform. However, notable differences in the shape and position of *O. wegneri* molariforms distinguish them from those of other mylodontines. The M1 of *P. harlani*, *G. robustum*, and *M. darwinii* are elongated anteroposteriorly, and their major axis is oriented following the divergence of the tooth rows. *Oreomylodon wegneri* is the only taxon that has an M1 with the major axis in variable orientations, often not aligned with the divergence of the tooth row. In some specimens of *O. wegneri*, the M1 is found to be outside the line described by the tooth row and the major axis of M1 is closely oblique to the tooth row, medially oriented, whereas in others the anterior edge of M1 is labially oriented. Similarly, the C1 is rotated in the maxilla in several specimens of *O. wegneri*, a unique condition within mylodontinae.

Morphogeometric Analysis of the Palate

Oreomylodon wegneri has the most distinctive palate configuration of all the ground sloths analyzed (Fig. 10B). This degree of morphological divergence is only reached by *M. darwinii* located at another end of the variation. The maxilla of *O. wegneri* resembles that of *Lestodon* because of the enormous anterior opening of the tooth rows; however, the absence in *O. wegneri* of an exaggerated diastema between C1 and M1 easily differentiates it. The Mio-Pliocene mylodontines *P. garbanii*, *G. chapadmalense*, and *S. uccasamamensis* are grouped in a defined sector of morphospace that allows us to recognize two primitive features shared by these three species: tooth rows anteriorly very divergent but very narrow toward M3–M4 and a small diastema between C1 and M1.

The morphological differences between the palates of *G. robustum* from the Pampean region and *P. harlani* in North America separate them completely except for one specimen of *G. robustum*, MNHN SGO.PV.2 from Chile (Püschel et al., 2017), that falls within the morphospace occupied by *P. harlani*. This specimen has divergent tooth rows, but they are almost straight, unlike the arched tooth rows at the level of the M2 of *G. robustum* of the Pampean region. In the same way, the holotype and the paratype

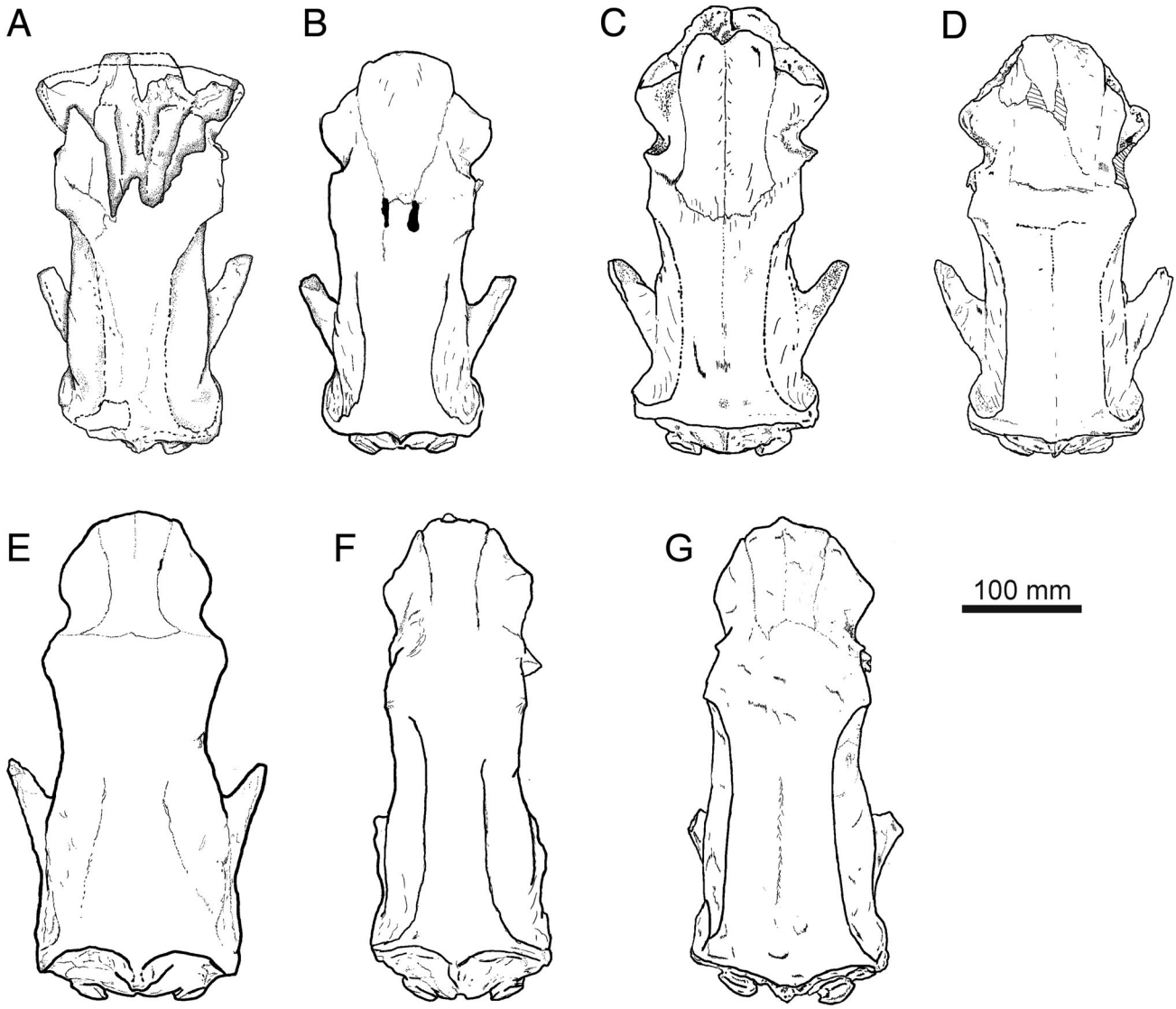

FIGURE 13. Mylodontid crania in dorsal view. **A**–**D**, *Oreomylodon wegneri*: **A**, MECN 417; **B**, EFM 01; **C**, EPNV-120; **D**, EPNV-5213. **E**, **F**, *Glossotherium robustum*: **E**, MLF 442; **F**, MLF 420. **G**, MARC 15675.a.2/244.

of *G. phoenesis* (Cartelle et al., 2019) are within the limits of the variation in *P. harlani* and far from *G. robustum*. Each tooth row of *G. phoenesis* is almost aligned as in *G. robustum* from Chile. Furthermore, not only the configuration of the teeth in the maxilla is shared by *G. phoenesis* and *P. harlani* but also the rounded shape of the occipitals of both species.

Oreomylodon wegneri and *G. robustum* near each other in the morphospace (Fig. 10), but this may reflect similarities in diet rather than a phylogenetic signal. Bargo et al. (2006) considered that *G. robustum* had a broad, semisquare muzzle, indicating a less selective grazing herbivore than other mylodontids such as *S. leptocephalum* or *M. darwinii*. The wider muzzle of *O. wegneri* may reflect a similar, bulk-feeding diet.

Nasal Morphology

The nasal region of *O. wegneri* is one of the most distinctive features among all mylodontids. The increase in size of the dorsal turbinals and dorsal meatus could also indicate increase of the olfactory epithelia. The dorsal meatus is ventrally well delimited in *O. wegneri* as a consequence of the ventral development of the dorsal nasal turbinal, unlike in *G. robustum* where the dorsal meatus and middle meatus are openly connected. This remarkable delimitation of areas in the vestibular region indicates separate respiratory and olfactory airflow paths in *O. wegneri*. Due to the size of the dorsal meatus, it is possible that a greater percentage of the inspired air was directed to constitute the olfactory airflow, which is driven to the chemosensory region, in comparison in *G. robustum*.

Additionally, the cone shape of the dorsal meatus could be an adaptation to concentrate odorant molecules in the air by capturing them anteriorly and driving them to olfactory epithelia in the ethmoturbinate region. In this way, the unique development of the dorsal region, only observed in *O. wegneri*, would have a positive impact on olfactory ability.

It has been proposed that at the end of the Pleistocene, there were conditions that altered the climate (Clapperton, 1987). South America reached its glacial maximum around 30 ka BP when sea and lake levels dropped, despite an increase in precipitation, and mean temperatures declined to between 5°C and 8°C (Ficcarelli et al., 1997; Van der Hammen, 1983; Van der Hammen

TABLE 1. Altitude range of localities with late Pleistocene mylodontines.

Taxon	Altitude (m)	Locality (minimum – maximum)	Reference
Glossotherium tropicorum	0–600	Santa Elena, Ecuador – Borja, Perú	De Iuliis et al., 2017
Lestodon armatus	0–900	Pampean region, Argentina – Nono, Córdoba, Argentina	This work
Glossotherium phoenesis	1,000	Toca dos Ossos, Ouro Branco, Bahia, Brazil	Cartelle et al., 2019
Glossotherium robustum	0–1,550	Pampean region, Argentina – Pampa Vaca Corral, Córdoba, Argentina	This work; Krapovickas et al., 2017
Glossotherium elmollarum	1,950	La Angostura, Tucumán, Argentina	Esteban, 1993
Mylodon darwinii	0–3,000	Pampean region, Argentina – Majotorillo, Bolivia	Favotti et al., 2015
Oreomylodon wegneri	2,450–3,100	La Armenia, Quito, Ecuador – Cusubamba, Cotopaxi, Ecuador	This work

and Absy, 1994). Clapperton (1987) and Porter (1981) suggest that the snow line in the northern and central Andes would have been 1,000 m lower than the current limit, with terminal moraines at 3,500 m altitude (Ficcarelli et al., 1997). The Cangagua Formation, which occurs between 1,900 and 3,000 m in elevation, contains the majority of *O. wegneri* remains and would have been deposited under these conditions. *Oreomylodon wegneri* shows specific adaptations to its singular environment (Hoffstetter, 1948, 1952, 1982; Román-Carrión, 2007). The large size of the vestibular region and the nasal atrium could be related to the high-altitude habitat of *O. wegneri*, which exceeds the altitudes of other mylodontines from the late Pleistocene (Table 1). These anatomical features could be an adaptive advantage to regulate body temperature and for the filtration and humidification of cold and dry air in the Ecuadorian Andes during the late Pleistocene (Fig. 14).

Phylogenetic Considerations

The phylogenetic analysis allows us to consider the novel evolutionary adaptations of *Oreomylodon wegneri*. The analysis showed that *O. wegneri* has a much closer position to *P. harlani*

FIGURE 14. Life reconstruction of a group of *Oreomylodon wegneri* in the inter-Andean valleys of Ecuador. Credits: Pablo Lara.

than to *G. robustum*. This challenges the old concept of *O. wegneri* as a synonym of *G. robustum* or even a member of the genus *Glossotherium*. Its closest relationship with other genera therefore justifies its assignment to a different subgenus (now genus) created by Hoffstetter (1949, 1952) and followed by Dechaseaux (1971). Additionally, the shape of the posterior edge of nasals of *O. wegneri* suggests that the species from the northernmost region of South America and those from North America share a common origin closer to each other than they are to the southern species of South America such as *G. robustum* and *G. chapadmalense*.

CONCLUSIONS

Oreomylodon wegneri shows remarkable differences from *Glossotherium robustum* that clearly negate its synonymy with this species or inclusion in the genus. The posterior shape of the nasals shows that *G. robustum* belongs to a lineage that evolved in the central region of Argentina at least from the Pliocene, whereas *O. wegneri* would be more related to other mylodontids such as *P. harlani* and *P. garbanii*. However, *Oreomylodon wegneri* differs markedly from all genera known. The more flared development of dorsal meatus in the nasal cavity, the morphology of the tooth rows, and the variability present in the degree of rotation of the major axis of the caniniform make it unique among the mylodontines and justify its taxonomic location within a distinct and endemic genus of Ecuador.

ACKNOWLEDGMENTS

We thank C. Montalvo (UCE), G. Medina and H. Román (INABIO), M. Espinosa (Museo Inst. Nac. Mejía), M. Reguero (MLP), A. A. Kramarz (MACN), G. Acuña and H. Arsani (MCA), E. Milicich, R. Paoletti, and staff of MLF, E. Aguirre (MPAHND), Y. Matos (MARC), M. L. Taglioretti and F. Scaglia (MMP), J. L. Ramírez (MMCIPAS), and M. Sioli (MRS) for facilitating access to collections; R. K. McAfee for images of crania of *P. harlani*; P. Lara, for his advice in the elaboration of the figures; and S. Bidart, M. Hidalgo, and staff of Biblioteca Florentino Ameghino, Facultad de Ciencias Naturales y Museo de La Plata, for providing relevant literature for this work. Secretary of Science and Technology of Universidad Nacional de Rosario helped finance this research. We thank editor E. Davis and reviewers H. G. McDonald and K. Prassack for comments that significantly improved the original manuscript.

ORCID

José Luis Román-Carrión http://orcid.org/0000-0003-0773-8393
Luciano Brambilla http://orcid.org/0000-0001-5670-7345

LITERATURE CITED

Arzani, H., S. L. Lanzelotti, G. E. A. Suárez, and N. M. Novo. 2014. Primer registro de pelos fósiles en *Glossotherium robustum* (Xenarthra, Mylodontidae), Pleistoceno Tardío, Mercedes, Provincia de Buenos Aires, Argentina. Ameghiniana 51:585–590.

Bargo, M. S., G. De Iuliis, and S. F. Vizcaíno. 2006. Hypsodonty in Pleistocene ground sloths. Acta Palaeontologica Polonica 51:53–61.

Boscaini, A., T. J. Gaudin, B. Mamani Quispe, P. Münch, P. O. Antoine, and F. Pujos. 2018a. New well-preserved craniodental remains of *Simomylodon uccasamamensis* (Xenarthra: Mylodontidae) from the Pliocene of the Bolivian Altiplano: phylogenetic, chronostratigraphic and palaeobiogeographical implications. Zoological Journal of the Linnean Society 185:459–486.

Boscaini, A., A. D. Iurino, G. Billet, L. Hautier, R. Sardella, G. Tirao, T. J. Gaudin, and F. Pujos. 2018b. Phylogenetic and functional implications of the ear region anatomy of *Glossotherium robustum* (Xenarthra, Mylodontidae) from the Late Pleistocene of Argentina. The Science of Nature. doi:10.1007/s00114-018-1548-y.

Brambilla, L., and D. A. Ibarra. 2018. The occipital region of late Pleistocene Mylodontidae of Argentina. Boletín del Instituto de Fisiografía y Geología 88:1–9.

Brambilla, L., and D. A. Ibarra. 2019. *Archaeomylodon sampedrinensis* gen. et sp. nov., a new mylodontine from the Middle Pleistocene of the Pampean Region, Argentina. Journal of Vertebrate Paleontology. doi:10.1080/02724634.2018.1542308.

Branco, W. 1883. Über Eine Fossile Säugethier-Fauna von Punin bei Riobamba in Ecuador. Beschreiburg der Fauna. Geologische und Paläontologische Abhandlungen 1:57–204.

Cartelle, C., G. De Iuliis, A. Boscaini, and F. Pujos. 2019. Anatomy, possible sexual dimorphism, and phylogenetic affinities of a new mylodontine sloth from the late Pleistocene of intertropical Brazil. Journal of Systematic Palaeontology. doi:10.1080/14772019.2019.1574406.

Clapperton, C. M. 1987. Glacial geomorphology. Quaternary glacial sequence and paleoclimatic inferences in the Ecuadorian Andes; pp. 843–870 in V. Gardiner (ed.), International Geomorphology 1986, Part II. Wiley, London.

Clavery, E. 1925. A propos de la découverte d'ossements de *Mylodon* à Cotocollao (Équateur). La Nature, n. 2689, Paris, pp. 244–245.

Coltorti, M., G. Ficcarelli, H. Jahren, M. Moreno-Espinosa, L. Rook, and D. Torre. 1998. The last occurrence of Pleistocene megafauna in the Ecuadorian Andes. Journal of South American Earth Sciences 11:581–586.

Cope, E. D. 1889. The Edentata of North America. American Naturalist 23:657–664.

Czerwonogora, A., and R. A. Fariña. 2012. How many Pleistocene species of *Lestodon* (Mammalia, Xenarthra, Tardigrada)? Journal of Systematic Palaeontology 11:251–263.

De Iuliis, G., T. J. Gaudin, and M. J. Vicars. 2011. A new genus and species of nothrotheriid sloth (Xenarthra, Tardigrada, Nothrotheriidae) from the late Miocene (Huayquerian) of Peru. Palaeontology 54:171–205.

De Iuliis, G., C. Cartelle, H. G. McDonald, and F. Pujos. 2017. The mylodontine ground sloth *Glossotherium tropicorum* from the late Pleistocene of Ecuador and Perú. Papers in Palaeontology 3:613–636.

Dechaseaux, C. 1971. *Oreomylodon wegneri*, Edente gravigrade du Pleistocene de l'Equateur—crane et moulage endocranien. Annales de Paleontologie 57:243–285.

Delsuc, F., F. M. Catzeflis, M. J. Stanhope, and E. J. P. Douzery. 2001. The evolution of armadillos, anteaters and sloths depicted by nuclear and mitochondrial phylogenies: implications for the status of the enigmatic fossil *Eurotamandua*. Proceedings of the Royal Society of London B: Biological Sciences 268:1605–1615.

Esteban, G. I. 1993. A new genus of Mylodontinae from the Pleistocene of northwestern Argentina (El Mollar, Tafí del Valle, Tucumán). Quaternary of South America and Antarctic Peninsula 8:29–37.

Esteban, G. I. 1996. Revisión de los Mylodontinae cuaternarios (Edentata-Tardigrada) de Argentina, Bolivia y Uruguay. Sistemática, filogenia, paleobiología, paleozoogeografía y paleoecología. Ph.D. dissertation, Universidad Nacional de Tucumán, Facultad de Ciencias Naturales e Instituto Miguel Lillo, Tucumán, Argentina, 314 pp.

Favotti, E., E. S. Ferrero, and D. Brandoni. 2015. Primer registro de *Mylodon darwini* Owen (Xenarthra, Tardigrada, Mylodontidae) en la Formación arroyo Feliciano (Pleistoceno tardío), Entre Ríos, Argentina. Revista Brasileira de Paleontologia 18:547–554.

Ficcarelli, G., M. Coltorti, M. Moreno-Espinosa, P. L. Pieruccini, L. Rook, and D. Torre. 2003. A model for the Holocene extinction of the mammal megafauna in Ecuador. Journal of South American Earth Sciences 15:835–845.

Ficcarelli, G., A. Azzaroli, A. Bertini, M. Coltorti, P. Mazza, C. Mezzabotta, and D. Torre. 1997. Hypothesis on the cause of extinction of the South American mastodonts. Journal of South American Earth Sciences 10:29–38.

Flower, W. H. 1883. On the arrangement of the orders and families of existing Mammalia. Proceedings of the Zoological Society of London 51:178–186.

Gaudin, T. J. 1995. The ear region of edentates and the phylogeny of the Tardigrada (Mammalia, Xenarthra). Journal of Vertebrate Paleontology 15:672–705.

Gaudin, T. J. 2004. Phylogenetic relationships among sloths (Mammalia, Xenarthra, Tardigrada): the craniodental evidence. Zoological Journal of the Linnean Society 140:255–305.

Gill, T. 1872. Arrangements of the families of mammals, with analytical tables. Smithsonian Miscellaneous Collections 11:1–98.
Goloboff, P., J. Farris, and K. Nixon. 2008. TNT, a free program for phylogenetic analysis. Cladistics 24:774–786.
Hoffstetter, R. 1948. Nota preliminar sobre los edentata xenarthra del Pleistoceno ecuatoriano. Boletín de Informaciones Científicas Ecuatorianas 2:19–42.
Hoffstetter, R. 1949. Nuevas observaciones sobre los Edentata del Pleistoceno Superior de la Sierra ecuatoriana. Boletín de Informaciones Científicas Ecuatorianas 3:67–99.
Hoffstetter, R. 1952. Les Mammifères Pléistocènes de la République de l'Equateur. Mémoires de la Société Géologique de France, Nouvelle Serie 31. Paris, 391 pp.
Hoffstetter, R. 1982. Les Edentés Xénarthres, un groupe singulier de la faune néotropicale (origine, affinités, radiation adaptative, migrations et extinctions). In: Montanaro Galitelli E (ed). Proceedings of the First International Meeting on "Palaeontology, Essential of Historical Geology" Venise: 385–443.
Kraglievich, L. 1925. Cuatro nuevos gravígrados de la fauna Araucana Chapadmalalense. Anales del Museo Nacional de Historia Natural de Buenos Aires 33:215–235.
Kraglievich, L. 1934. Contribución al conocimiento de *Mylodon darwini* Owen y especies afines. Revista del Museo de La Plata 34:255–292.
Krapovickas, J. M., A. A. Tauber, and A. Haro. 2017. Quaternary biostratigraphy and biogeography of mountain region of Córdoba, Argentina. Geobios 50:211–236.
McAfee, R. K. 2009. Reassessment of the cranial characters of *Glossotherium* and *Paramylodon* (Mammalia: Xenarthra: Mylodontidae). Zoological Journal of the Linnean Society 155:885–903.
McDonald, H. G. 2005. Paleoecology of extinct xenarthrans and the Great American Biotic Interchange. Bulletin of the Florida Museum of Natural History 45:313–333.
McDonald, H. G., and G. De Iuliis. 2008. Fossil history of sloths; pp. 39–55 in Sergio F. Vizcaíno and W. J. Loughry (eds.), The Biology of the Xenarthra. University Press of Florida, Gainesville, Florida.
Montellano-Ballesteros, M., and J. L. Román-Carrión. 2011. Redescubrimiento de material tipo depositado en la colección del Museo de Historia Natural 'Gustavo Orcés V.' del Instituto de Ciencias Biológicas, Escuela Politécnica Nacional, Quito, Ecuador. Boletín de la Sociedad Geológica Mexicana 63:379–392.
Owen, R. 1842. Description of the skeleton of an extinct gigantic sloth, *Mylodon robustus*, OWEN, with observations on the osteology, natural affinities, and probable habits of the megatherioid quadruped in general. R. and J. E. Taylor, London. 176. pp.
Pascual, R., M. G. Vucetich, G. J. Scillato-Yané, and M. Bond. 1985. Main pathways of mammalian diversification in South America; pp. 219–247 in F. G. Stehli and S. D. Webb (eds.), The Great American Biotic Interchange. Plenum Press, New York.
Patterson, B., W. Segall, W. D. Turnbull, and T. J. Gaudin. 1992. The ear region in xenarthrans (= Edentata, Mammalia). Part II. Pilosa (sloths, anteaters), palaeanodonts, and a Miscellany. Fieldiana Geology, new series 24:1–79.
Pitana, V. G., G. I. Esteban, A. M. Ribeiro, and C. Cartelle. 2013. Cranial and dental studies of *Glossotherium robustum* (Owen, 1842) (Xenarthra: Pilosa: Mylodontidae) from the Pleistocene of southern Brazil. Alcheringa 37:147–162.
Porter, S. C. 1981. Pleistocene glaciation in the southern Lake District of Chile. Quaternary Research 24:269–292.
Püschel, H. P., T. A. Püschel, and D. Rubilar-Rogers. 2017. Taxonomic comments of a *Glossotherium* specimen from the Pleistocene of central Chile. Boletín del Museo Nacional de Historia Natural de Chile 66:223–262.
Rinderknecht, A., E. Bostelmann, D. Perea, and G. Lecuona. 2010. A new genus and species of Mylodontidae (Mammalia: Xenarthra) from the late Miocene of southern Uruguay, with comments on the systematics of the Mylodontinae. Journal of Vertebrate Paleontology 30:899–910.
Robertson, J. S. 1976. Latest Pliocene mammals from Haile XVA, Alachua County, Florida: Bulletin of the Florida State Museum, Biological Sciences, v. 20, p. 111 –186.
Román-Carrión, J. L. 2007. Nuevos datos sobre la distribución geográfica de los "perezosos gigantes" del Pleistoceno del Ecuador. Politécnica 27:111–124.
Román-Carrión, J. L. 2012a. Hallazgo de megafauna pleistocénica en el centro histórico de Quito. Revista Politécnica 30:136–146.
Román-Carrión, J. L. 2012b. Registro de fauna pleistocénica en Caraburo, nor-oriente de Quito. Revista Politécnica 30:205–210.
Scillato-Yané, G. J. 1977. Octomylodontinae: nueva subfamilia de Mylodontidae (Edentata, Tardígrada). Descripción del cráneo y mandíbula de *Octomylodon robertoscagliai* n. sp., procedentes de la Formación Arroyo Chasicó (Edad Chasiquense, Plioceno temprano) del sur de la Provincia de Buenos Aires (Argentina). Algunas consideraciones filogenéticas y sistemáticas sobre los Mylodontoidea. Publicaciones del Museo Municipal de Ciencias Naturales 2:123–140.
Slater, G. J., P. Cui, A. M. Forasiepi, D. Lenz, K. Tsangaras, B. Voirin, N. de Moraes-Barros, R. D. E. MacPhee, and A. D. Greenwood. 2016. Evolutionary relationships among extinct and extant sloths: the evidence of mitogenomes and retroviruses. Genome Biology and Evolution 8:607–621.
Spillmann, F. 1931. Die Säugetiere Ecuadors im Wandel der Zeit (I. Teil). Universidad Central, Quito, Ecuador, 112 pp.
Stock, C. 1907. Further observations on the skull structure of mylodont sloths from Rancho La Brea. University of California Press, Bulletin of the Department of Geology 10:165–178.
Van der Hammen, T. 1983. Palaeocology and palaeogeography of savannas; pp. 19–35 in F. Bourliere (ed.), Ecosystems of the World, no. 13. Elsevier Science Publication Company, Amsterdam, The Netherlands.
Van der Hammen, T., and M. L. Ahsy. 1994. Amazonia during the last glacial. Palaeogeography Palaeoclimatology Palaeoecology 109:247–261.
Wagner, A. 1860. Ueber fossile Säugthierknochen am Chimborasso. Sitzungsberichte der königl. bayerischen Akademie der Wissenschaften., Munchen, pp. 330–338.

Submitted May 8, 2019; revisions received September 6, 2019;
accepted September 8, 2019.
Handling editor: Edward Davis.

APPENDIX 1. List of character states for *Oreomylodon wegneri* used in the TNT analysis of the data matrix of Gaudin (2004).

	10	20	30	40	50	60
Oreomylodon wegneri	1201101020	20[02]21[13]0111	2001010[01]0[01]	134[34]74[23]000	2[12]0110201?	10[01]0222211
	70	80	90	100	110	120
	1300022101	001100????	03003331111	0000101110	1011001101	0013111??0
	130	140	150	160	170	180
	4311110002	1012221010	0000310000	0011101201	1201000301	0113100010
	190	200	210	220	230	240
	02000[01]100[01]	211[12]010?00	0100100?00	0020001111	??1?0?1?10	11111201[01]0
	250	260	270	280	286	
	11?0101111	?211011232	0[12]21111012	0????02[01]11	102101	